Approximation of pore space with ellipsoids: a comparison of a geometrical method with a statistical one.

Lucie Druoton, Dominique Michelucci, Olivier Monga, Abdelaziz Bouras

Approximation of pore space with ellipsoids: a comparison of a geometrical method with a statistical one.

1st Lucie Druoton
LE2I laboratory
University of Burgundy
Dijon, France
lucie.druoton@u-bourgogne.fr

2nd Dominique Michelucci
LE2I laboratory
University of Burgundy
Dijon, France
dominique.michelucci@u-bourgogne.fr

3rd Olivier Monga
IRD
University of Paris 6
Bondy, France
olivier.monga@ird.fr

4th Abdelaziz Bouras
DCSE,College of Engineering
Qatar University
Qatar
abdelaziz.bouras@qu.edu.qa

***Abstract*—We work with tomographic images of pore space in soil. The images have large dimensions and so in order to speed-up biological simulations (as drainage or diffusion process in soil), we want to describe the pore space with a number of geometrical primitives significantly smaller than the number of voxels in pore space. In this paper, we use the curve skeleton of a volume to segment it into some regions. We describe the method to compute the curve skeleton and to segment it with a simple segment approximation. We approximate each obtained region with an ellipsoid. The set of final ellipsoids represents the geometry of pore space and will be used in future simulations. We compare this method which we call geometrical method with the one described in the paper [8], which we name statistical method (using k-means algorithm).**

***Index Terms*—Pore space approximation; ellipsoids; curve skeleton; segmentation;**

I. Introduction

In recent years, much progress has been made on tomographic images of porous media, particularly in soil sciences. Images are more and more large and accurate, making biological and drainage simulations long and complex using voxel approaches. Some works are already existing on the representation of the geometry of the pore space of soils to decrease the number of primitives to be treated and thus to reduce the computation time of these simulations. We work on improving that and describing the geometry of the poral space using the techniques of image analysis and 3d-modeling.

The goal of our work is to represent 3D shapes from voxel-based representation using primitives like ellipsoids [2]–[4]. In [8], [13], the voxels set is approached with the smallest set of maximal spheres covering the pore space. This set is calculated using Delaunay triangulation. The spheres are centered on the surface skeleton of the shape: they are maximal spheres contained in the shape. The centers of these spheres sample the surface skeleton of the shape. In [8], [12], [15], this set of spheres is approximated with a set of geometric primitives. In [12], [15] these primitives are cylinders, whereas in [8] they are ellipsoids. Compared to spheres and cylinders, ellipsoids better fit pore space cavities. Moreover, we can still extract from these primitives a diameter value, needed in Young-Laplace equation for drainage simulation. So the use of ellipsoids seems to be a good choice, for our applications, according to primitive complexity and error fitting.

The algorithm given in [8] has two steps. The first one consists in clustering the set of maximal spheres using segmentation methods and the second step consists in merging the computed primitives in the case where they overlap too much. In our work, we aim at simplifying this algorithm by removing its second step: indeed, if the segmentation method gives a better set of ellipsoids, it is no more needed to merge the primitives at the end. Hence, we proceed by studying different segmentation methods. The one used in [8] is the k-means algorithm, see also [11].

The pore space is extracted (with some thresholding) from tomographic 3D images of significant size. The pore space is initially a huge set of voxels. To speed-up physical simulations of drainage and diffusion in soils, a more compact representation of the poral space is essential. The simulation will be done on a graph the vertices of which represent the different regions of the pore space, and the edges of which join two neighboring regions. The information of the volume of each region will be stored on the corresponding vertex. An opening value will be calculated between two neighboring regions and will represent the exchange capacity between two regions. This information and the distance between the centers of each region will be stored on the corresponding edge. When the simulation is performed on a 3D matrix of voxels, this graph is implicit. Simulation calculations are essentially the same on both graphs. We expect that the simulation on the regions graph will be more efficient than on the voxels graph, without loss of precision.

Our work focused on the study of 3D image segmentation methods preserving the geometry and topology.

We consider the pore space as a volume V bordered by a connected surface S. The surface S has no border, and separates an interior (of finite volume in the bounding box of S) and an exterior (of infinite volume). The volume V represents all the voxels of the pore space. When the surface S is not connected, we decompose it into connected components.

We consider a voxel indexed by the triple (i, j, k) as the real point of coordinates (i, j, k).

The method described in [8] uses the maximal spheres centered in the region bordered by the surface S. So, we have studied the literature on segmentation of surface skeleton and curve skeleton of a surface S.

Several methods of calculation of the surface skeleton (or medial axis) are given in the literature [1], [21] but there are few methods of segmentation of the surface skeleton, see [17].

In [21], the authors compute a distance map (or distance field) by solving an eikonal equation (of light ray trajectory) using the Fast-Marching method. From this map, the skeleton points are extracted using the Laplacian. In [1], the authors describe the Power Crust algorithm that approaches the medial axis of a point cloud using the Voronoi diagram (or equivalently the Delaunay triangulation) and permits to reconstruct the surface from this skeleton. In [17], the authors segment the 3D skeleton of a volume using its 2D boundaries.

There are also different discrete or continuous curve skeleton extraction methods [5], [20], [22]. The paper [5] describes the homotopic thinning algorithm. In [22], the authors adapt this algorithm in the particular case of tubular surfaces representing blood vessels for medical diagnostics. Still in a medical application, in [20], the authors calculate an iterative contraction of a mesh to obtain the curve skeleton.

Papers [19] and [18] compare different methods for computing curve skeletons. [19] gives a comparison of mesh contraction based methods with geometric criteria such as homotopy, thickness, preservation of details whereas [18] focuses on voxel-based methods. Several articles deal with a 3D surface segmentation based on the segmentation of the curve skeleton [6], [16].

The paper [16] deals with surface segmentation using the critical points of the curve skeleton and using the geodesic distance (the length of the shortest paths inside the volume V) to segment the volume attached to the skeleton, whereas in [6] the authors present a mesh segmentation algorithm. They first transform the mesh into a voxel representation and then, they calculate the curve skeleton by homotopic thinning using the skeleton as a graph. Each branch of the graph (or skeleton) is then associated with a region of the segmentation.

Our work is inspired by this last method, starting directly from the voxel representation of a connected region of the pore space. We determine the curve skeleton by homotopic thinning (described in particular in [5]).

The points (or voxels) of the boundary of the volume are iteratively deleted as long as their removal does not change the topology of the volume (number of connected components, Euler characteristic). A condition is added to preserve the geometrical features of the object: a point cannot be deleted when it has only one neighbor (it prevents to reduce the skeleton to a single point for a convex volume).

We use the curve skeleton of a volume to segment the poral space into several regions. Each region can be approximated with an ellipsoid. The curve skeleton contains all the information of the geometry of a volume, this is why, in this paper, we call it the geometric method, in order to differentiate it from Kemgue and Monga's method, [8]. The latter uses the k-means algorithm which clusters several data in k regions. This algorithm is used on the centers of maximal spheres contained in the volume. The geometric information lies in these maximal spheres. Since the k-means algorithm is often used in statistics, we call this method, in this paper, the statistical method. We compare our results with this method on the same images.

In the following paragraphs, we describe the method of extraction of the curve skeleton, paragraph II and then, we describe how we segment this skeleton with a simple polygonal approximation, paragraph III.

In paragraph IV, we give the geometric results and compare with the statistical method described in [8] before the merging step.

Finally, we conclude on the efficiency of the two methods and give our perspectives of work to ameliorate and use the geometrical method in the context of drainage and diffusion simulations.

II. Extracting the discrete curve skeleton of a 3D image

We work with Matlab software in which several toolboxes enable the manipulation of 3D images as matrix. The pore space V is extracted with some thresholding from tomographic 3D images. Then, we use the homotopic thinning method to compute the curve skeleton, [9]. A voxel (i, j, k) can be deleted if all the following conditions hold, [10]:

- It is on the boundary of the volume V, i.e. at least one of its 26 neighbors is outside V.
- It is not an ending point (An ending point has only one neighbor), with the 26-neighborhood.
- Its suppression does not modify the Euler characteristics (topological condition).
- Its suppression does not modify the number of connected components.

We obtain the results presented in the following figures, Fig 1 on synthetic data and Fig. 2 and Fig. 3 on real data. The red dots are the skeleton points and the initial surface is in transparent gray. Note that we work separately on each connected component of the poral space V.

III. From skeleton points to graph, segmentation and ellipsoid approximation

This section deals with the curve skeleton segmentation and the approximation of pore space by a set of ellipsoids.

The curve skeleton is used as a graph in which each node is a point (or voxel) of the curve skeleton. We consider the 26-neighborhood of the voxels. The curve skeleton has by construction thickness 1. There are different kinds of nodes, depending on their degree: the number of neighbors, Fig. 4. The ending nodes are nodes with only one neighbor. They are at the extremity of branches. The simple nodes are nodes with exactly two neigbours. The interior nodes are nodes with more than two neigbors. They are the nodes at the intersection of

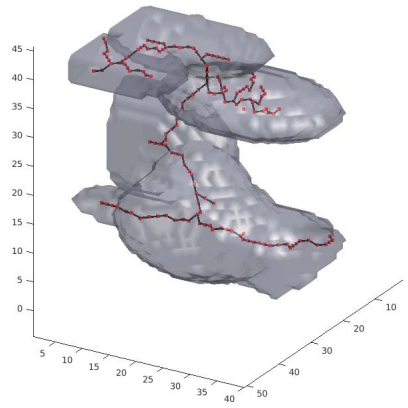

Fig. 1. Representation of the points of the curve skeleton on a synthetic 3D image representing pore space (with a unique connected component). Red dots are skeleton points.

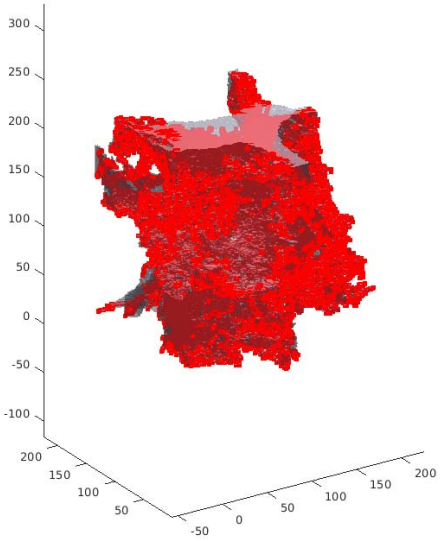

Fig. 2. Representation of the points of the curve skeleton on the biggest connected component of a real 3D image from tomography of soil. Red dots are skeleton points.

branches. A branch is a maximal set of neighboring simple nodes. The graph is black on the figure Fig. 1.

First, we segment the graph in a set of branches between two nodes that are not simple nodes, that is to say node with a degree different of 2. We suppose here that the graph is not reduced to a cycle. Secondly, a set of segments are computed on each branch. From a node of the branch, we determine the vector that goes to the last node and so on. While we go to the same direction, the nodes are on the same segment, otherwise we define a new segment, see Fig. 5.

Then, each voxel of V, including boundary voxels, is associated to the nearest segment of the curve skeleton: it gives a partition of voxels of V. To do that, we use the

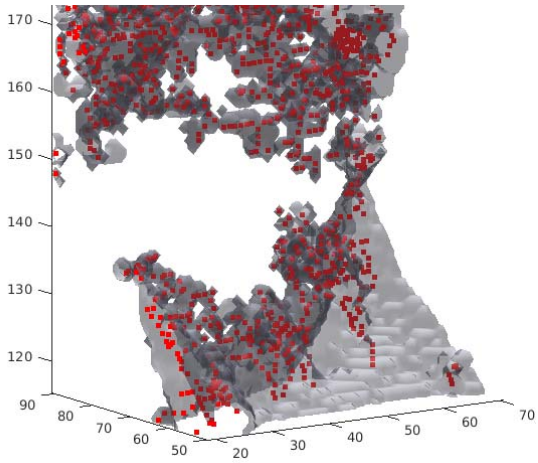

Fig. 3. Zoom of the points of the curve skeleton of the Fig. 2.

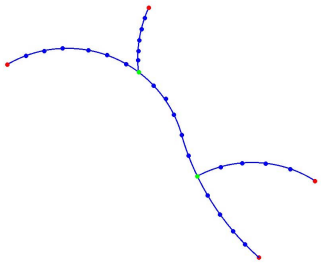

Fig. 4. Representation of different kinds of nodes in the skeleton graph. In green, interior nodes. In red, ending nodes. In blue, simple nodes.

Dijkstra's algorithm which computes the shortest paths inside V between the source (all skeleton points) and the other points of V. These paths do not exit the volume V; it would happen using for example an Euclidean distance on a non-convex part of V. The length of these shortest paths is called the geodesic distance. On Fig. 7, the color of a point is the color of its closer skeleton segment. It defines a region per segment of the curve skeleton. To finish, we determine a bounding ellipsoid per region, see Fig. 8, using the volume minimization method [14]. We could as well compute the best ellipsoid (its axis are the eigenvectors of the covariance matrix [2]), or the closest ellipsoid (the ellipsoid the closest to boundary points of the region, with some least square method). Finally, we could also test the ellipsoids-free approach, i.e. compute volumes (counting voxels in each region) and gravity centers of regions, opening values (counting voxels "between" two regions), distances between two neighboring regions, and use these values for the graph.

IV. Comparison of the geometrical method with the statistical one

In this section, we give our results and compare them to results of the method described by Kemgue and Monga [8].

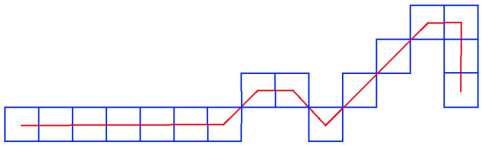

Fig. 5. An example of simple polygonal approximation on a branch of a curve skeleton. In blue, the voxels of the curve skeleton and in red the segments.

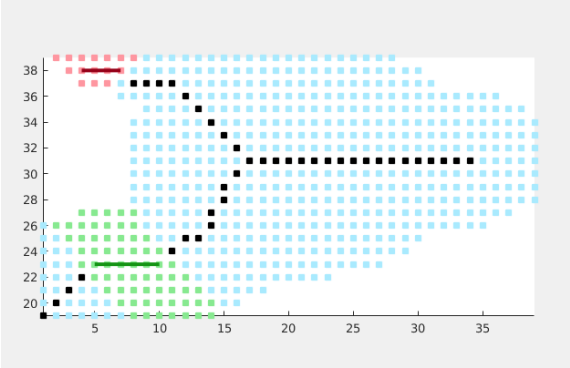

Fig. 6. An example in 2D of two regions. In red the voxels of the region associated to the red segment, in green the voxels of the region associated to the green segment. In black the other voxels of the curve skeleton and in blue the other voxels of the pore space.

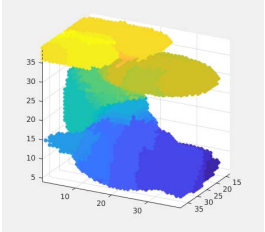

Fig. 7. Illustration of regions using the simple polygonal approximation of the curve skeleton. The curve skeleton is the one on the Fig. 1.

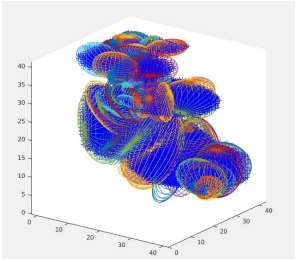

Fig. 8. The set of bounding ellipsoids determined by the volume minimization method.

Algorithm 1 Approximation of the pore space by a set of ellipsoids using the k-means algorithm

Input: a set of voxels representing the pore space

- computation of maximal spheres centered in the pore space (approximation of the surface skeleton)
- segmentation in k class, k fixed, with the k-means algorithm applied on the centers of maximal spheres
- for each class, computation of the convex hull of the union of the maximal spheres of the class and approximation by an ellipsoid.
- computation of the error. If the error is above the threshold, increase k and reiterate from the second point above.

Output: a set of ellipsoids approaching the pore space

The first method detailed in algorithm 1 is the statistical method described by Kemgue and Monga [8]. The second method detailed in algorithm 2 is the geometrical method using curve skeletons described previously in paragraph II and III.

We compare the two methods first on synthetic images representing the pore space and secondly on real images (only on the biggest connected component for visibility). We compare the results before the merging step that we want to suppress. We define the following geometrical criteria for the evaluation of the algorithms:

- the error of reconstruction: the volume of the symmetric difference between the initial poral volume and the reconstructed one. The volume is measured counting voxels.

- the number of ellipsoids (or the number of regions).

- the intersection volume of the ellipsoids, which should be as small as possible. The volume is measured counting voxels.

- the mean of minimal, medial and maximal radii of ellipsoids. This criterion verifies if large pores and small pores are differentiated by the used method.

As the first algorithm is iterative, we fix its maximum error threshold to the value obtained with the second method. Results are given on Table I and II. We obtain Fig. 9 on synthetic data and Fig. 10 and 11 on real data.

Algorithm 2 is faster than algorithm 1 : the computation times of the curve skeleton and the maximal spheres are equivalent, but finding an ellipsoid fitting a set of points is much faster than finding an ellipsoid fitting a set of spheres. In the second case, it is necessary to compute a set of points in the convex hull of the discretisation of the set of spheres before fitting these points by an ellipsoid.

The volume of superposition of ellipsoids are equivalent in the two algorithm.

We can see also that in general, with algorithm 1, the different regions have almost the same size and we can not make a difference between large and little pores. For our applications in drainage and diffusion, it is fundamental to distinguish large pores from little ones. For example, in drainage process, for a given pressure the little pores are filled with water whereas the largest ones are filled with air.

Considering only symmetrical difference, algorithm 1 is more flexible than algorithm 2 because it is iterative. So it is possible to control the symmetrical difference error adjusting the number of ellipsoids. In its current state, algorithm 2 is not iterative, the number of regions is fixed because it depends on the segmentation of the curve skeleton. If needed, we can make it iterative halving segments and fixing a minimum number of voxels per region.

V. Conclusion and Future Works

This paper presents a comparison between two algorithms for fitting pore space with ellipsoids. For future simulations of drainage and diffusion, we have to distinguish large pores from little ones. We propose an algorithm using the segmentation of the curve skeleton of the pore space to put ellipsoids. We call this method the geometric method and compare it to the one exposed in [8] that we call statistical method (because it uses k-means algorithm).

Algorithm 2 Approximation of the pore space using segmentation of the curve skeleton

Input: a set of voxels representing the pore space

- computation of the curve skeleton by the thinning method
- computation of the graph representing the curve skeleton
- segmentation into branches
- polygonal approximation of each branch: determination of a set of segments
- for each segment, determination of the nearest points of the volume (with Dijkstra's algorithm)
- approximation of these points by an ellipsoid.

Output: a set of ellipsoids approaching the pore space

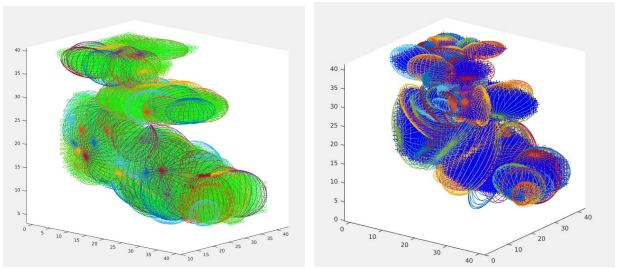

Fig. 9. Results of algorithms 1 (left) and 2 (right) on the example of the Fig.2.

According to our criteria, this method gives good results but it has to be validated in the simulations of drainage and diffusion, which is the objective of our project (work in progress). In case it is needed to improve this description of the pore space (in our applications or for other uses), we now give some tracks that can be explored later.

The first is that ellipsoids are not the only primitives that can be used to approximate the regions obtained by the geometrical method. We could use the superellipsoids [7], more general than ellipsoids and allowing a better fitting to the regions. It is possible to find the best parameters of a superellipsoid fitting a set of points using, for example, Levenberg-Marquardt or BFGS algorithm.

We could also directly use each region as a set of voxels (a list of voxels) for drainage and diffusion simulations. By directly using the region segmentation of the geometric method, we eliminate the symmetric difference of approximation of poral space with maximal spheres or ellipsoids because we keep all the initial voxels.

Moreover, with the statistical method, the poral space is approximated by a set of ellipsoids. It is then necessary to calculate a graph describing this set. Each ellipsoid is represented by a vertex and two overlapping ellipsoids give an edge in the graph. This graph is necessary for simulations. In the geometric method, the graph is directly obtained from the graph of the curve skeleton, so it is no longer necessary to calculate it.

Finally, in order to validate with results of physical simulations, we will test the best geometrical representation (superellipsoids or regions) with simulation of drainage and diffusion on real images. We will compare with Lattice-Boltzmann (voxels-based) simulations, which give the ground-truth.

TABLE I
COMPARATIVE TABLE OF ALGORITHM 1 AND 2 ON THE EXAMPLE OF THE FIG.9.

	Algorithm 1	Algorithm 2
nb of voxels in pore space	13162	13162
nb of maximal spheres or skeleton voxels	3731	150
nb of ellipsoids	70	105
symmetrical difference	30%	38%
volume of superposition of ellipsoids	89%	86%
mean of minimal radii (standard deviation)	$3.46(\pm 0.89)$	$2.57(\pm 1.14)$
mean of medial radii (standard deviation)	$4.44(\pm 0.55)$	$4.29(\pm 1.57)$
mean of maximal radii (standard deviation)	$5.30(\pm 0.48)$	$6.46(\pm 1.88)$
computation time	$140s$	$55s$

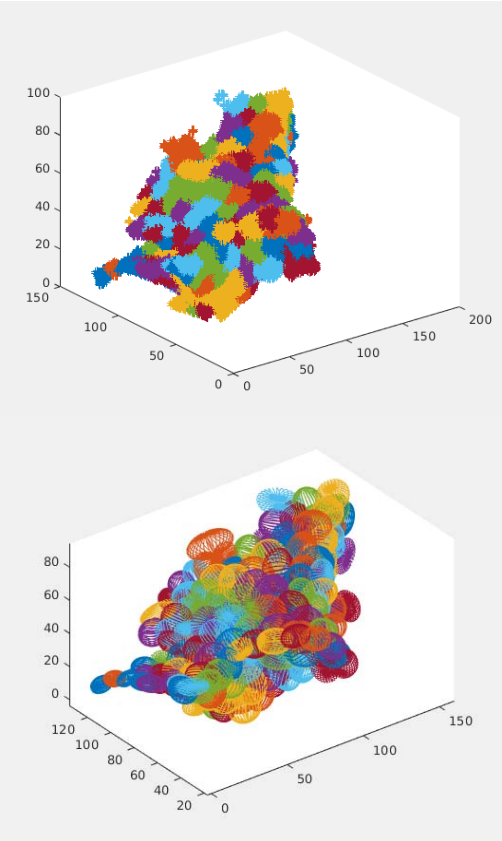

Fig. 10. Results of algorithm 1 on a real image of pore space. The regions obtained by k-means algorithm (top). The points are points in maximal spheres on each region. The ellipsoids approximating the previous regions (bottom).

ACKNOWLEDGMENT

This publication was made possible by NPRP grant #9-390-1-088 from the Qatar National Research Fund. The findings achieved herein are solely the responsibility of the authors.

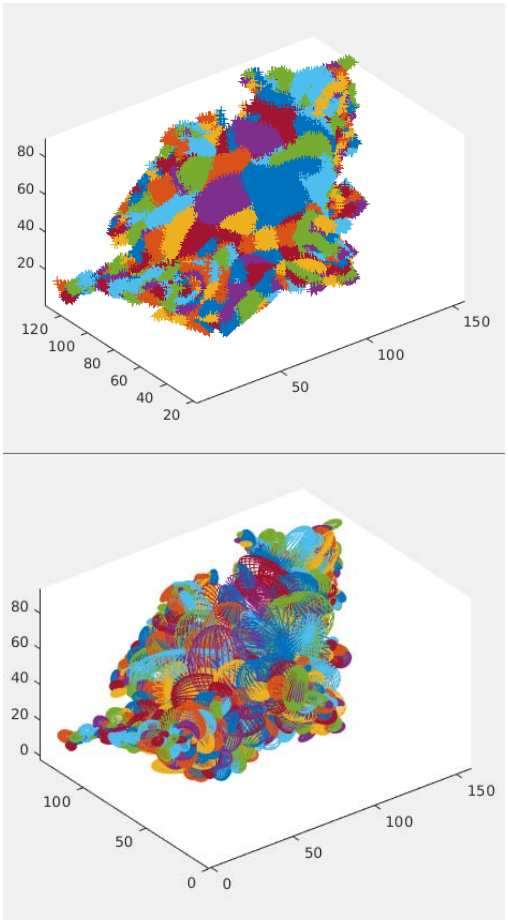

Fig. 11. Results of algorithm 2 on a real image of pore space. The regions obtained by segmenting the curve skeleton (top). The ellipsoids approximating the previous regions (bottom).

TABLE II
COMPARATIVE TABLE OF ALGORITHM 1 AND 2 ON THE EXAMPLE OF FIG.10 AND FIG.11.

	Algorithm 1	Algorithm 2
nb of voxels in pore space	269640	269640
nb of maximal spheres or skeleton voxels	111203	4162
nb of ellipsoids	218	726
symmetrical difference	40%	48%
volume of superposition of ellipsoids	74%	87%
mean of minimal radii (standard deviation)	$7.30(\pm 1.71)$	$3.20(\pm 2.04)$
mean of medial radii (standard deviation)	$8.54(\pm 1.58)$	$4.81(\pm 3.03)$
mean of maximal radii (standard deviation)	$9.95(\pm 1.66)$	$7.36(\pm 4.39)$
computation time	$740s$	$373s$

REFERENCES

[1] AMENTA, N., CHOI, S., AND KOLLURI, R. K. The power crust. In *Proceedings of the sixth ACM symposium on Solid modeling and applications* (2001), ACM, pp. 249–266.

[2] BANÉGAS, F., JAEGER, M., MICHELUCCI, D., AND ROELENS, M. The ellipsoidal skeleton in medical applications. In *Proceedings of the sixth ACM symposium on Solid modeling and applications* (2001), ACM, pp. 30–38.

[3] BANEGAS, F., MICHELUCCI, D., ROELENS, M., AND JAEGER, M. An automatic adaptive surface reconstruction from ellipsoidal skeleton. In *Implicit surfaces'99. Fourth International Workshop on Implicit Surfaces, ENSERB, Universit de Bordeaux 1, Talence, 13-15 septembre 1999, J. Hughes, C. Schlick (eds)* (1999), pp. 113–122.

[4] BANEGAS, F., MICHELUCCI, D., ROELENS, M., AND JAEGER, M. Hierarchical automated clustering of cloud point set by ellipsoidal skeleton: application to organ geometric modeling from ct-scan images. In *Medical Imaging 1999: Image Processing* (1999), vol. 3661, International Society for Optics and Photonics, pp. 1227–1238.

[5] BERTRAND, G., AND COUPRIE, M. Transformations topologiques discretes. In *Gomtrie discrte et images numriques, David Coeujolly, Annick Montanvert et Jean-Marc Chassery* (2007), Hermes, pp. 187–209. chapter 8 in book Gomtrie discrte et images numriques, David Coeujolly, Annick Montanvert et Jean-Marc Chassery, pages 187-209, Herms, 2007.

[6] BRUNNER, D., AND BRUNNETT, G. Mesh segmentation using the object skeleton graph. In *Proc. IASTED International Conf. on Computer Graphics and Imaging* (2004), pp. 48–55.

[7] CHEVALIER, L., JAILLET, F., AND BESKURT, A. Segmentation et modlisation 3d par un ensemble de superellispodes. *Revue internationnale d'ingnierie numrique 1*, 3 (2005), 311–336.

[8] KEMGUE, A. T., AND MONGA, O. From voxels to ellipsoids: Application to pore space geometrical modelling. In *IT Convergence and Security 2017*. Springer, 2018, pp. 184–193.

[9] KERSCHNITZKI, M., KOLLMANNSBERGER, P., BURGHAMMER, M., DUDA, G., WEINKAMER, R., WAGERMAIER, W., AND FRATZL, P. Architecture of the osteocyte network correlates with bone material quality. *Journal of Bone and Mineral Research 28*, 8 (2013), 1837–1845.

[10] LEE, T.-C., KASHYAP, R. L., AND CHU, C.-N. Building skeleton models via 3-d medial surface axis thinning algorithms. *CVGIP: Graphical Models and Image Processing 56*, 6 (1994), 462–478.

[11] MOKHTARI, B., MELKEMI, K., MICHELUCCI, D., AND FOUFOU, S. Dynamic clustering-based method for shape recognition and retrieval. In *TMCE 2014, Tools and Methods of Competitive Engineering, May 1923, 2014, Budapest, Hungary* (May 2014).

[12] MONGA, O. Defining and computing stable representations of volume shapes from discrete trace using volume primitives: Application to 3d image analysis in soil science. *Image and Vision Computing 25*, 7 (2007), 1134–1153.

[13] MONGA, O., BOUSSO, M., GARNIER, P., AND POT, V. 3d geometric structures and biological activity: Application to microbial soil organic matter decomposition in pore space. *Ecological Modelling 216*, 3-4 (2008), 291–302.

[14] MOSHTAGH, N. Minimum volume enclosing ellipsoid. In *http://www.mathworks.com/matlabcentral/fileexchange/9542* (2006).

[15] NGOM, N. F., MONGA, O., MOHAMED, M. M. O., AND GARNIER, P. 3d shape extraction segmentation and representation of soil microstructures using generalized cylinders. *Computers & geosciences 39* (2012), 50–63.

[16] RENIERS, D., AND TELEA, A. Skeleton-based hierarchical shape segmentation. In *Shape Modeling and Applications, 2007. SMI'07. IEEE International Conference on* (2007), IEEE, pp. 179–188.

[17] RENIERS, D., AND TELEA, A. Segmenting simplified surface skeletons. In *International Conference on Discrete Geometry for Computer Imagery* (2008), Springer, pp. 262–274.

[18] SOBIECKI, A., JALBA, A., AND TELEA, A. Comparison of curve and surface skeletonization methods for voxel shapes. *Pattern Recognition Letters 47* (2014), 147–156.

[19] SOBIECKI, A., YASAN, H. C., JALBA, A. C., AND TELEA, A. C. Qualitative comparison of contraction-based curve skeletonization methods. In *International Symposium on Mathematical Morphology and Its Applications to Signal and Image Processing* (2013), Springer, pp. 425–439.

[20] WANG, S., WU, J., WEI, M., AND MA, X. Robust curve skeleton extraction for vascular structures. *Graphical Models 74*, 4 (2012), 109–120.

[21] XIA, H., AND TUCKER, P. G. Distance solutions for medial axis transform. In *Proceedings of the 18th International Meshing Roundtable*. Springer, 2009, pp. 247–265.

[22] ZWETTLER, G., PFEIFER, F., SWOBODA, R., AND BACKFRIEDER, W. Accelerated skeletonization algorithm for tubular structures in large datasets by randomized erosion. In *VISAPP (1)* (2008), pp. 74–81.